

Graph Sampling Based Deep Metric Learning for Generalizable Person Re-Identification

Shengcai Liao*

Inception Institute of Artificial Intelligence (IIAI)
Masdar City, Abu Dhabi, UAE

scliao@ieee.org

Ling Shao

Terminus Group
China

ling.shao@ieee.org

Abstract

Recent studies show that, both explicit deep feature matching as well as large-scale and diverse training data can significantly improve the generalization of person re-identification. However, the efficiency of learning deep matchers on large-scale data has not yet been adequately studied. Though learning with classification parameters or class memory is a popular way, it incurs large memory and computational costs. In contrast, pairwise deep metric learning within mini batches would be a better choice. However, the most popular random sampling method, the well-known PK sampler, is not informative and efficient for deep metric learning. Though online hard example mining has improved the learning efficiency to some extent, the mining in mini batches after random sampling is still limited. This inspires us to explore the use of hard example mining earlier, in the data sampling stage. To do so, in this paper, we propose an efficient mini-batch sampling method, called graph sampling (GS), for large-scale deep metric learning. The basic idea is to build a nearest neighbor relationship graph for all classes at the beginning of each epoch. Then, each mini batch is composed of a randomly selected class and its nearest neighboring classes so as to provide informative and challenging examples for learning. Together with an adapted competitive baseline, we improve the state of the art in generalizable person re-identification significantly, by 25.1% in Rank-1 on MSMT17 when trained on RandPerson. Besides, the proposed method also outperforms the competitive baseline, by 6.8% in Rank-1 on CUHK03-NP when trained on MSMT17. Meanwhile, the training time is significantly reduced, from 25.4 hours to 2 hours when trained on RandPerson with 8,000 identities. Code is available at <https://github.com/ShengcaiLiao/QAConv>.

1. Introduction

Person re-identification is a popular computer vision task, where the goal is to find a person, given in a query image, from the search over a large set of gallery images. In the last two years, generalizable person re-identification has gain increasing attention due to both its research and practical value [12, 13, 18, 22, 27, 47, 49]. This task studies the generalizability of a learned person re-identification model in unseen scenarios, and employs direct cross-dataset evaluation [10, 39] for performance benchmarking.

For deep metric learning, beyond feature representation learning and loss designs, explicit deep feature matching schemes are shown to be effective for matching person images [1, 15, 18, 25, 29], due to the advantages in addressing pose and viewpoint changes, occlusions, and misalignments. In particular, a recent method, called query-adaptive convolution (QAConv) [18], has proved that explicit convolutional matching between gallery and query feature maps is quite effective for generalizable person re-identification. However, these methods all require more computational costs compared to conventional feature learning methods.

Beyond novel generalizable algorithms, another way to improve generalization is to enlarge the scale and diversity of the training data. For example, a recent dataset called RandPerson [34] synthesized 8,000 identities, while [32] and [2] both collected 30K persons for re-identification training. These studies all observed improved generalization ability for person re-identification. However, the efficiency of deep metric learning from large-scale data has not yet been adequately studied in person re-identification.

There are some popular ways of learning deep person re-identification models, including classification (with the ID loss [44]), metric learning (with a pairwise loss [5, 39] or triplet loss [9]), and their combinations (e.g. ID + triplet loss). Using an ID loss is convenient for classification learning. However, in large-scale deep learning, involving classifier parameters incurs large memory and computational costs in both the forward and backward passes. Similarly,

*Shengcai Liao is the corresponding author.

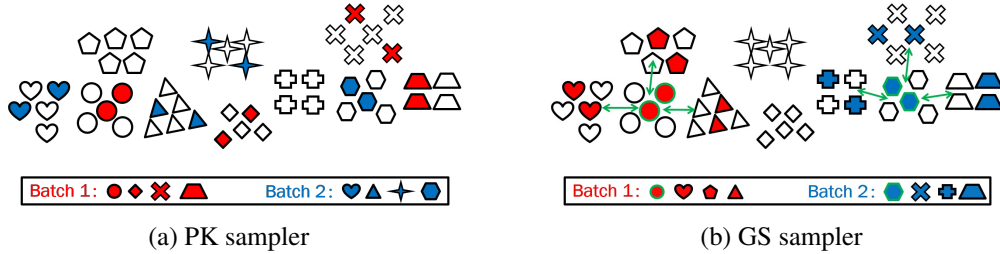


Figure 1. Two different sampling methods: (a) PK sampler; and (b) the proposed GS sampler. Different shapes indicate different classes, while different colors indicate different batches. GS constructs a graph for all classes and always samples nearest neighboring classes.

involving class signatures for metric learning in a global view is also not efficient. For example, QACConv in [18] is difficult to scale up for large-scale training, because a class memory module is designed, where full feature maps are stored for all classes as signatures, and they are required for cross feature map convolutional matching during training.

Therefore, involving class parameters or signatures in either classification or metric learning is not efficient for large-scale person re-identification training. In contrast, we consider that pairwise deep metric learning between samples in mini batches is better suited for this task. Accordingly, the batch sampler plays an important role for efficient learning [9, 38]. The well-known PK sampler [9, 23] is the most popular random sampling method in person re-identification. It first randomly selects P classes, and then randomly samples K images per class to construct a mini batch of size $B = P \times K$. Since this is performed randomly, the sampled instances within a mini batch are uniformly distributed across the whole dataset (see Fig. 1 (a)), and might therefore not be informative and efficient for deep metric learning. To address this, an online hard example mining method was proposed in [9], which improved the learning efficiency to some extent. However, the mining is performed online on the already sampled mini batches. Therefore, this method is still limited by the fully random PK sampler, because the mini batches obtained by this sampler do not consider the sample relationship information.

To address this, we propose to shift the hard example mining earlier to the data sampling stage. Accordingly, we propose an efficient mini-batch sampling method, called graph sampling (GS), for large-scale deep metric learning. The basic idea is to build a nearest neighbor relationship graph for all classes at the beginning of each epoch. Then, the mini-batch sampling is performed by randomly selecting a class as anchor, and its top- k nearest neighboring classes, with the same K instances per class, as shown in Fig. 1 (b). This way, instances within a sampled mini batch are mostly similar to each other, so as to provide informative and challenging examples for discriminant learning. From face recognition loss function studies [4, 20, 36], it is known that focusing on boundary (hard) examples helps improving

the discriminant ability of the learned model, and helps resulting in compact representations that generalize well beyond the training data. The GS sampler shares a similar idea in focusing on nearest neighboring classes, and thus has a potential of improving the discrimination and generalization ability of the learned model.

In summary, the contributions of this paper include: (1) We propose a new mini-batch sampling method, termed GS, and prove that it enables more efficient learning than the well-known PK sampler; (2) We improve a very competitive baseline by 6.8% in Rank-1 with MSMT17 \rightarrow CUHK03-NP, and reduce the training time significantly, from 25.4 hours to 2 hours on RandPerson with 8,000 identities; and (3) Together with the baseline, we improve the state of the art in generalizable person re-identification significantly, by 20.6% in Rank-1 with Market-1501 \rightarrow MSMT17, and by 25.1% in Rank-1 with RandPerson \rightarrow MSMT17.

2. Related Work

Metric learning approaches have been widely studied in the early stage of person re-identification. Many algorithms have been proposed, such as the well-known PRDC [45], KISSME [14], and XQDA [17], to name a few. In recent years, deep metric learning in particular has become popular and been extensively studied. Beyond feature representation learning, specific deep metric learning can be roughly classified in terms of loss function designs and deep feature matching schemes. For loss function designs, pairwise loss functions [5, 39], classification or identification loss [44], and triplet loss [9, 23, 45] are the most popular. For deep feature matching schemes, a number of methods have been proposed in the literature. For example, Ahmed et al. proposed a deep convolutional architecture with layers specifically designed for local neighborhood matching [1]. Li et al. proposed a novel filter pairing neural network (FPNN) to jointly handle several known challenges, such as misalignment and occlusions [15]. Shen et al. proposed an end-to-end deep Kronecker-Product Matching (KPM) network [25] for softly aligned matching. Suh et al. proposed a deep neural network to learn part-aligned bilinear representations [29]. Liao and Shao proposed the query-adaptive

convolution (QAConv) for explicit deep feature matching, and proved its effectiveness for generalizable person re-identification [18]. They also proposed a Transformer based method, TransMatcher [19], for improved performance.

Generalizable person re-identification was initially studied in [10, 39], where direct cross-dataset evaluation was proposed to benchmark algorithms. With advancements in deep learning, this task has gained increasing attention in recent years. For example, Song et al. [27] proposed a domain-invariant mapping network with a meta-learning pipeline. Jia et al. [12] adopted both instance and feature normalization to alleviate both style and content variances across datasets. Zhou et al. proposed a new backbone network called OSNet [47], and further demonstrated its advantages in generalizing deep models [47]. Jin et al. proposed a style normalization and restitution module, which shows good generalizability [13]. Yuan et al. proposed an adversarial domain-invariant feature learning network (ADIN), which explicitly learns to separate identity-related features from challenging variations [40]. Zhuang et al. proposed a camera-based batch normalization (CBN) method for domain-invariant representation learning [49]. Recently, meta-learning has also been shown to be effective for learning generalizable models. For example, Zhao et al. proposed memory-based multi-source meta-learning (M³L) for generalizing to unseen domains [42]. Choi et al. proposed the MetaBIN algorithm for meta-training the batch-instance normalization network [3]. Bai et al. proposed a dual-meta generalization network and a large-scale dataset called Person30K for person re-identification [2]. In addition to the above, Wang et al. proposed a large-scale synthetic person re-identification dataset, called RandPerson, and proved that models learned from synthesized data generalize well to real-world datasets [34].

However, the generalization of current methods is still far from satisfactory for practical person re-identification. Taking face recognition as a good example in practice, future directions may gradually be learning from more large-scale data for better performance. However, the efficiency of large-scale learning has been inadequately studied in person re-identification. As basic as the mini-batch sampler, though it plays an important role in deep metric learning [9, 37, 38], it still has not yet been much studied.

Beyond online hard example mining within mini batches [9], several methods have been proposed for hard example mining during data sampling for mini batches. Suh et al. [28] proposed a stochastic class-based hard example mining for deep metric learning. It uses learnable class signatures to find nearest classes, and further performs an instance-level refined search within the subset of classes found in the first stage for hard example mining. Besides, the Doppelganger [26] also relies on classification layers for doppelganger mining from the predicted classification

scores. However, these methods require classification parameters to be learned for class mining, which is intractable for large-scale classes and complex non-Euclidean matchers (e.g. QAConv). In [31], all training classes are divided into subspaces by clustering on averaged class representations, and then mini batches are sampled within each subspace. This method requires a full forward pass of all the training data, and the clustering operation cannot easily be scaled up to large-scale classes. In [7], SmartMining was proposed, which builds an approximate nearest neighbor graph for all training samples after a full forward pass of the training data for feature extraction. However, this instance-level mining can be very expensive in computation, and even infeasible for complex non-Euclidean metric layers. In contrast, we propose and prove that sampling one example per class for class mining works well for large-scale deep metric learning without classification or instance-level mining.

3. Deep Metric Learning

There are two popular ways for learning deep person re-identification neural networks. The first one is the classification based method [44], also known as using the identification loss, or ID loss. This is a straightforward extension from general image classification. Since person re-identification is an open-class problem, the learned classifier is usually dropped after training. The last feature embedding layer is usually adopted instead (known as the identity embedding, or IDE [44]), and the Euclidean or cosine distance is applied to measure the distance between two person images. The second one is the triplet loss based method [9, 24], which is usually combined with the ID loss. Together with the online hard example mining, the triplet loss is a very useful auxiliary loss function for enhancing the discriminability of the learned model.

However, the above methods always require classifier parameters, which incur large memory and computational costs in both the forward and backward passes of large-scale deep learning. When dot products are employed for classification this is still acceptable to some extent. However, with more complex modules, e.g. QAConv [18] where a full feature map convolution is required for matching, learning with class signatures is difficult to scale up.

Therefore, for large-scale deep metric learning, we consider removing classification layers. Accordingly, pairwise matching between mini-batch samples is another solution [16, 39]. We adopt QAConv as our baseline method, which is the recent state of the art for generalizable person re-identification. It constructs query adaptive convolutional kernels on the fly for image matching, which suits pairwise learning. However, the original design of QAConv learning is based on the so-called class memory, which stores one feature map for each class for image-to-class matching, instead of using pairwise matching between mini-batch sam-

ples. Considering the matching complexity of the QAConv layer, this is not efficient in large-scale learning. Therefore, we only consider pairwise matching between mini-batch samples for QAConv, and remove its class memory.

4. Graph Sampling

4.1. Motivation

As discussed, for deep metric learning, the well-known PK sampler [9] is typically used to provide mini-batch samples. However, its random nature makes the sampled instances not informative enough for discriminant learning. In the PK sampler, as shown in Fig. 1 (a), P classes and K images per class are randomly sampled for each mini batch. Though an online hard example mining (OHEM) was further proposed in [9] to find informative instances within a mini batch, the PK sampler itself is still not efficient, as it provides limited hard examples for OHEM to mine.

Therefore, the sampling method itself needs to be improved so as to provide informative samples for mini batches. Instead of using fully random sampling, the relationships among classes need to be considered. Thus, we construct a graph for all classes at the beginning of each epoch, and always sample nearest neighboring classes in a mini batch so as to enable discriminant learning. We call this idea graph sampling (GS), which is detailed below.

4.2. GS Sampler

At the beginning of each epoch, we utilize the latest learned model to evaluate the distances or similarities between classes, and then construct a graph for all classes. This way, the relationships between classes can be used for informative sampling. Specifically, we randomly select one image per class to construct a small sub-dataset. Then, the feature embeddings with the current network are extracted, denoted as $\mathbf{X} \in R^{C \times d}$, where C is the total number of classes for training, and d is the feature dimension. Next, pairwise distances between all the selected samples are computed, e.g. by QAConv. As a result, a distance matrix $dist \in R^{C \times C}$ for all classes is obtained.

Then, for each class c , the top $P - 1$ nearest neighboring classes can be retrieved, denoted by $\mathcal{N}(c) = \{x_i | i = 1, 2, \dots, P - 1\}$, where P is the number of classes to sample in each mini batch. Accordingly, a graph $G = (V, E)$ can be constructed, where $V = \{c | c = 1, 2, \dots, C\}$ represents the vertices, with each class being one node, and $E = \{(c_1, c_2) | c_2 \in \mathcal{N}(c_1)\}$ represents the edges.

Finally, for the mini-batch sampling, for each class c as anchor, we retrieve all its connected classes in G . Then, together with the anchor class c , we obtain a set $A = \{c\} \cup \{x | (c, x) \in E\}$, where $|A| = P$. Next, for each class in A , we randomly sample K instances per class to generate a mini batch of $B = P \times K$ samples for training. A

pseudocode of the GS sampler is shown in Appendix A.

Note that, different from other mini-batch sampling methods, for the GS sampler the number of mini batches or iterations per epoch is always C , which is independent to the parameters B , P , and K . Nevertheless, the parameter B still affects the computational load of each mini batch. Besides, one may worry that the GS sampler will be computationally expensive. However, note that, firstly, only one image per class is randomly sampled for the graph construction; and, secondly, the above computation is performed only once per epoch. In practice, we find that the GS sampler with QAConv, which is already a heavy matcher compared to the mainstream Euclidean distance, only requires tens of seconds for thousands of identities. Details will be presented in the experimental section.

4.3. Loss Function

With mini batches provided by the GS sampler, we apply QAConv to compute similarity values between each pair of images, and formulate a triplet-based ranking learning problem within mini batches. Accordingly, we compute the batch OHEM triplet loss [9] alone for metric learning:

$$\ell(\theta; X) = \sum_{i=1}^P \sum_{a=1}^K [m - \min_{p=1 \dots K} s(f_{\theta}(x_i^a), f_{\theta}(x_i^p)) + \max_{\substack{j=1 \dots P \\ j \neq i \\ n=1 \dots K}} s(f_{\theta}(x_i^a), f_{\theta}(x_j^n))]_+, \quad (1)$$

where $X = \{x_i^a, i \in [1, P], a \in [1, K]\}$ contains the mini-batch samples, θ is the network parameter, f_{θ} is the feature extractor, $s(\cdot, \cdot)$ is the similarity, and m is the margin.

Note that Eq. (1) is usually used as an auxiliary to the ID loss, but not alone in person re-identification. This is probably because random samplers including PK cannot provide informative mini batches for OHEM to mine, which makes Eq. (1) very small or even zero, and so the learning is not efficient. In contrast, with the proposed GS sampler, we prove that the OHEM triplet loss works well by itself.

4.4. Gradient Clipping

Note that the GS sampler already provides almost the hardest mini batches, and the batch OHEM triplet loss further finds the hardest triplets within a mini batch for training. As a result, the model may suffer optimization difficulty, which in turn may impact convergence during training. In practice, we find that limiting $K = 2$ alleviates this problem significantly. Or otherwise, the binary cross-entropy loss for pairwise matching can be a more stable alternative to the OHEM triplet loss (see Appendix B).

Furthermore, to stabilize the training with the GS sampler and the hard triplet loss, we clip the gradient norm during the backward propagation. Specifically, let \mathbf{g} be the gradient of all parameters, and $\|\mathbf{g}\|$ be its norm. The gradient

will be clipped as $\mathbf{g} \leftarrow \min(1, \frac{T}{\|\mathbf{g}\|}) \cdot \mathbf{g}$, where T is a predefined threshold. That is, if the gradient norm is larger than T then clip it to be T . Note that GS and OHEM provide the hardest examples, which facilitates discriminant learning. However, this may also lead to overfitting. Therefore, besides stabilizing the training, the gradient clipping operation is also useful to regularize noisy gradients to avoid overfitting on source domain, and, in turn, improving the generalization performance. The effect of this gradient clipping will be analyzed in the experiments.

5. Experiments

5.1. Implementation Details

Our implementation is adapted from the official PyTorch code of QAConv [18] (MIT license). We first build an improved baseline based on QAConv. Specifically, ResNet-50 [8] is used as the backbone, with IBN-b layers appended, following several recent studies [12, 13, 21, 47, 49]. The layer3 feature map is used, with a neck convolution of 128 channels appended as the final feature map. The input image size is 384×128 (see Appendix E for results with 256×128). Several commonly used data augmentation methods are applied, including random cropping, flipping, occlusion [18], and color jittering. The batch size is set to 64. The SGD optimizer is adopted to train the network, with a learning rate of 0.0005 for the backbone, and 0.005 for newly added layers. The maximal learning epochs are 60. When the initial loss is reduced as a factor of 0.7, the learning rates are decayed by 0.1, and an early stopping is triggered after a further half of the already learned epochs. Gradient clipping is applied with $T = 8$. Automatic Mixed Precision (AMP) in PyTorch is applied to accelerate training. When the proposed GS sampler is further applied (denoted by QAConv-GS), we use the hard triplet loss ($m=16$), instead of the class memory based loss proposed in [18], and the default parameters for GS are $B=64$, and $K=2$.

5.2. Datasets

Four large-scale person re-identification datasets, CUHK03 [15], Market-1501 [43], MSMT17 [35], and RandPerson [34] are used in our experiments. The CUHK03 dataset contains 1,360 persons and 13,164 images. The most challenging subset named detected is used for our experiments. Besides, the CUHK03-NP protocol [46] is adopted, with 767 and 700 subjects used for training and testing, respectively. The Market-1501 dataset includes 32,668 images of 1,501 identities captured from six cameras. The training subset contains 12,936 images from 751 identities, while the test subset includes 19,732 images from 750 identities. The MSMT17 dataset contains 4,101 identities and 126,441 images captured from 15 cameras. It is divided into a training set of 32,621 images

from 1,041 identities, and a test set with the remaining images from 3,010 identities. The RandPerson dataset is a recently released synthetic person re-identification dataset. It contains 8,000 persons and 1,801,816 images. We use the subset including 132,145 images of the 8,000 identities. This dataset is only used for large-scale training and generalization testing. Cross-dataset evaluation [10, 39] is performed on all datasets, by training on the training subset of one dataset (except that with MSMT17 we further used an additional setting with all images for training), and evaluating on the test subset of another dataset. Rank-1 and mean average precision (mAP) are used as the performance metrics, evaluated under single-query evaluation protocol.

5.3. Comparison to the State of the Art

A comparison to the state of the art (SOTA) in generalizable person re-identification is shown in Table 1, where three datasets are used for training, and three others are used for testing. Note that, with MSMT17 as the training set, one setting is to use all images for training, regardless of its subset splits. This is denoted by MSMT17 (all). Several generalizable person re-identification methods published recently are compared, including OSNet-IBN [47], OSNet-AIN [48], MuDeep [22], SNR [13], QAConv [18], CBN [49], ADIN [40], and M³L [42]. Table 1 shows that QAConv-GS significantly improves the previous SOTA. For example, with Market-1501 \rightarrow CUHK03, the Rank-1 and mAP are improved by 8.8% and 9.0%, respectively. With Market-1501 \rightarrow MSMT17, they are improved by 20.6% and 7.7%, respectively. With MSMT17 (all) \rightarrow Market-1501, the improvements are 9.8% for Rank-1 and 13.8% for mAP. With RandPerson as the training data, the improvements on Market-1501 are 12% for Rank-1 and 7.4% for mAP, while the improvements on MSMT17 are 25.1% for Rank-1 and 8.7% for mAP. Though RandPerson is synthetic, the results show that models learned on it generalize quite well to real-world datasets, which confirms the findings in [34].

Note that, M³L [42] uses a different evaluation protocol, and thus the results are not directly comparable. Specifically, M³L is trained on three datasets selected from CUHK03, Market-1501, DukeMTMC-reID¹, and MSMT17, while the other is held for testing. Impressive results are obtained by M³L on CUHK03-NP, which, though not directly comparable, exceed all our results, including those trained with all MSMT17 images. However, on Market-1501, the proposed method trained on MSMT17 outperforms M³L in Rank-1 by 3.2%, while the mAPs are comparable. Furthermore, on MSMT17, the proposed method trained on Market-1501 significantly outperforms M³L, with 9% gain in Rank-1 and 2.5% in mAP. This is quite encouraging, since in both cases our training dataset is a subset of that used by M³L.

¹It is no longer available, so we do not use it in our experiments.

Method	Venue	Training	CUHK03-NP		Market-1501		MSMT17	
			Rank-1	mAP	Rank-1	mAP	Rank-1	mAP
M ³ L [42]	CVPR'21	Multi	33.1	32.1	75.9	50.2	36.9	14.7
MGN [22, 33]	ACMMM'18	Market-1501	8.5	7.4	95.7	86.9	-	-
MuDeep [22]	TPAMI'20	Market-1501	10.3	9.1	95.3	84.7	-	-
QAConv [18]	ECCV'20	Market-1501	9.9	8.6	-	-	22.6	7.0
OSNet-AIN [48]	TPAMI'21	Market-1501	-	-	94.2	84.4	23.5	8.2
CBN [49]	ECCV'20	Market-1501	-	-	91.3	77.3	25.3	9.5
QAConv-GS	Ours	Market-1501	19.1	18.1	91.6	75.5	45.9	17.2
PCB [30, 40]	ECCV'18	MSMT17	-	-	52.7	26.7	-	-
MGN [33, 40]	ACMMM'18	MSMT17	-	-	48.7	25.1	-	-
ADIN [40]	WACV'20	MSMT17	-	-	59.1	30.3	-	-
SNR [13]	CVPR'20	MSMT17	-	-	70.1	41.4	-	-
CBN [49]	ECCV'20	MSMT17	-	-	73.7	45.0	72.8	42.9
QAConv-GS	Ours	MSMT17	20.9	20.6	79.1	49.5	79.2	50.9
OSNet-IBN [47]	CVPR'19	MSMT17 (all)	-	-	66.5	37.2	-	-
OSNet-AIN [48]	TPAMI'21	MSMT17 (all)	-	-	70.1	43.3	-	-
QAConv [18]	ECCV'20	MSMT17 (all)	25.3	22.6	72.6	43.1	-	-
QAConv-GS	Ours	MSMT17 (all)	27.6	28.0	82.4	56.9	-	-
RP Baseline [34]	ACMMM'20	RandPerson	13.4	10.8	55.6	28.8	20.1	6.3
CBN [41]	ECCV'20	RandPerson	-	-	64.7	39.3	20.0	6.8
QAConv-GS	Ours	RandPerson	18.4	16.1	76.7	46.7	45.1	15.5

Table 1. Comparison of the state-of-the-art direct cross-dataset evaluation results (%). MSMT17 (all) means all images are used for training, regardless of subset splits. M³L is trained on three datasets selected from CUHK03, Market-1501, DukeMTMC-reID, and MSMT17, while the other is held for testing. Results in gray cells are with within-dataset evaluation for a reference. “-” means not reported or not applicable.

5.4. Ablation Study

5.4.1 Comparison of QAConv variants

Table 2 shows a comparison among different variations of QAConv: the original QAConv [18] (denoted as Ori), the competitive QAConv baseline we adapted (denoted as Base), and the proposed QAConv-GS. It shows that, beyond the successful learning scheme of the class memory module proposed in QAConv, QAConv-GS with the proposed GS sampler is also very effective in learning discriminant models. QAConv-GS outperforms the competitive baseline for all experiments, by 6.8% and 5.4% in Rank-1, respectively, on CUHK03 and Market-1501 when trained on MSMT17.

Interestingly, Table 2 also shows that the within-dataset evaluation results are also improved by QAConv-GS compared to the baseline. However, improving performance on a single dataset does not always lead to better generalization, since it may also overfit a dataset, as can be observed in Table 1. Therefore, we suggest a focus on generalization since it is more critical for practical applications.

Furthermore, we also compare the training time of QAConv (with class memory) and QAConv-GS. Both methods are tested on a single NVIDIA V100 GPU. From the comparison shown in Table 2, it can be observed that the original QAConv learned with class memory becomes very

	Training		CUHK03		Market		MSMT17	
	Data	Hours	R1	mAP	R1	mAP	R1	mAP
Ori	Market	1.33	9.9	8.6	-	-	22.6	7.0
Base	Market	0.47	14.6	14.6	88.7	71.4	42.6	15.8
GS	Market	0.25	19.1	18.1	91.6	75.5	45.9	17.2
Base	MSMT	1.33	14.1	15.7	73.7	44.7	72.5	43.4
GS	MSMT	0.73	20.9	20.6	79.1	49.5	79.2	50.9
Ori	MS-all	26.9	25.3	22.6	72.6	43.1	-	-
Base	MS-all	15.0	23.4	23.1	80.1	53.2	-	-
GS	MS-all	3.42	27.6	28.0	82.4	56.9	-	-
Base	RP	25.4	15.2	14.6	75.9	46.0	44.4	15.5
GS	RP	2.0	18.4	16.1	76.7	46.7	45.1	15.5

Table 2. Comparison of QAConv variants. Ori: the original QAConv [18]. Base: the competitive baseline we adapted. GS: graph sampling (ours). MS-all: MSMT17 (all). RP: RandPerson.

slow when trained on large-scale datasets, such as the full MSMT17 or RandPerson. This is not surprising, because in each mini-batch iteration, the QAConv with class memory needs to compute matching scores between mini-batch samples and the feature map memory of all classes; and the number of classes is 4,101 in MSMT17, and 8,000 in Rand-

Person. In contrast, the proposed pairwise learning with the GS sampler is much more efficient because it avoids matching all classes in each iteration. As can be seen from Table 2, the training time of the baseline QAConv can be reduced from 25.4 hours to 2 hours when trained on RandPerson with 8,000 identities, which is a significant achievement.

In addition, we also evaluate the sampling efficiency of the proposed GS sampler. As stated earlier, it constructs a graph at the beginning of each epoch. We evaluate the running time of all the computations in GS. The results are 4 seconds on Market-1501, 9 seconds on the MSMT17 training subset, 40 seconds on the full MSMT17 dataset, and 138 seconds on RandPerson with 8,000 identities. Therefore, the GS sampler is in fact efficient, despite being incorporated into QAConv, which is a heavy matcher compared to the mainstream Euclidean distance.

5.4.2 Comparison of different sampling methods

In Table 3, using the same QAConv and hard triplet loss, we compare three mini-batch sampling methods, including PK, a clustering based method [31] (denoted as Cluster), and GS. Besides, the implementation of PK and Cluster follows GS, where the number of batches per epoch is determined by the number of classes. For [31], since k-means does not support non-Euclidean metric, we replace it with spectral clustering. The subspace parameter M in [31] is set to 10, after an optimization in [5, 50]. From Table 3, we can see that PK performs the worst, due to its fully random nature, which does not provide enough hard examples in mini batches. Besides, we can see that, with the subspace clustering method proposed in [31], the performance is generally improved, thanks to the more informative mini batches sampled within each cluster. However, feature extraction from the whole training set and clustering of all classes are time consuming. In contrast, the proposed GS sampler is more efficient, since it only considers one example per class for the graph construction. Furthermore, GS also achieves the best performance, with improvements over Cluster of up to 4.7% in Rank-1, and 3.4% in mAP. We believe that clustering is less effective than graph based GS due to two reasons. First, only cluster centers may be surrounded by their dense neighbors, while others, especially boundary points (classes), may not be always with their full set of neighbors in the same cluster. Second, mini-batch classes need to be randomly sampled within a cluster, of which the operation may further miss out some nearest neighbors of each class.

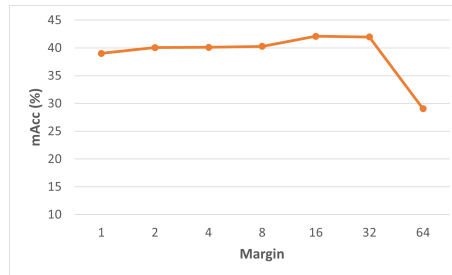
Furthermore, in Appendix C, applications to two other baselines, OSNet [47] and TransMatcher [19], also verify the generality of GS’s advantage over PK. Besides, application to unsupervised domain adaptation (UDA) with GS in SpCL [6] is discussed in Appendix D, and a variant of GS using class centers is analyzed in Appendix E.

Method	Training		CUHK03		Market		MSMT17	
	Data	Time	R1	mAP	R1	mAP	R1	mAP
PK	Market	99	17.9	17.0	-	-	43.3	15.6
	Cluster	117	18.4	17.3	-	-	44.0	15.8
	GS	100	19.1	18.1	-	-	45.9	17.2
PK	MSMT	141	18.6	18.8	75.7	46.1	-	-
	Cluster	196	18.4	19.2	77.2	47.6	-	-
	GS	145	20.9	20.6	79.1	49.5	-	-
PK	MS-all	669	24.5	24.6	78.7	52.1	-	-
	Cluster	881	26.3	26.3	80.4	54.2	-	-
	GS	685	27.6	28.0	82.4	56.9	-	-
PK	RP	1,150	16.9	14.7	73.2	43.5	40.3	13.1
	Cluster	1,922	17.3	15.0	73.3	43.3	40.4	13.4
	GS	1,397	18.4	16.1	76.7	46.7	45.1	15.5

Table 3. Comparison of different sampling methods. MS-all: MSMT17 (all). RP: RandPerson. Time is with seconds per epoch.



(a) Effect of batch size B



(b) Effect of margin m

Figure 2. mAcc (%) performance with (a) different batch sizes, and (b) different margin parameters, trained on MSMT17.

5.4.3 Parameter analysis

In Fig. E, we show the performance of the proposed method with different batch sizes and margin parameters. The training is performed on MSMT17. For ease and reliable comparison, we report the average (denoted by mAcc) of all Rank-1 and mAP results on all test sets over four random runs. We observe that, generally, the accuracy increases with increasing batch size B , but saturates at 64. As for the margin parameter m , note that the QAConv similarity score $s(\cdot, \cdot)$ used in Eq. (1) ranges in $(-\infty, +\infty)$. Fig. E(b) shows

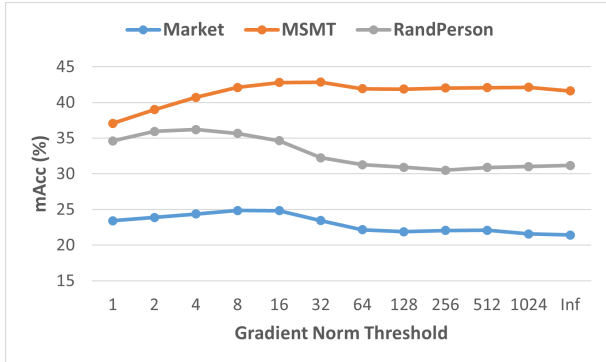


Figure 3. Influence of gradient clipping, trained on three datasets.

that the performance slightly improves with increasing m due to the increased discriminability, and achieves the best with $m=16$. However, after $m=32$, the performance drops significantly, due to intractable learning difficulty.

5.4.4 Effect of gradient clipping

Next, we study the effect of gradient clipping on the learning of QAConv-GS. The results are shown in Fig. 3. Interestingly, when trained on MSMT17, the performance is less affected without gradient clipping (Inf). Specifically, with gradient clipping, only a slight improvement can be obtained, but too small threshold T even prevent effective model learning. This is because, in our experiments, MSMT17 is the most comprehensive dataset. It provides large-scale and diverse training examples, which prevents overfitting in the view of “regularization from data”. However, with the small-scale training dataset Market-1501, and the quite different synthetic dataset RandPerson, gradient clipping does provide useful regularization for model training, and improves the generalization performance. Therefore, a reasonable value of $T=8$ is considered as a trade-off.

5.4.5 Visualization of GS

Fig. F shows some examples (more in Appendix F) of the nearest neighboring classes generated by the GS sampler. As can be observed, the GS sampler is indeed able to find similar classes as hard examples to challenge the learning. For example, it identifies similar kinds of clothes, colors, patterns, and accessories. These confusing examples help a lot in learning discriminative models.

6. Conclusion

With this study, we show that the popular PK sampler is not efficient in deep metric learning, and thus we propose a new batch sampler, called the graph sampler, to help learning discriminant models more efficiently. This is achieved



(a) Market-1501



(b) MSMT17

Figure 4. Groups of examples of the nearest neighboring classes generated by the GS sampler when trained on (a) Market-1501 and (b) MSMT17. In each group, the upper left image is the center class, and other images are the top-7 nearest neighboring classes.

by constructing a nearest neighbor graph of all classes for informative sampling. Together with a competitive baseline, we achieve the new state of the art in generalizable person re-identification with a significant improvement. Meanwhile, the training time is much reduced by removing the classification parameters and only using the pairwise distances between mini batches for loss computation. We believe the proposed technique is general and may also be applied in other fields, such as image retrieval, and face recognition, among others. Moreover, we discuss social impacts and some limitations of this research in Appendix G and H.

Acknowledgements

Special thanks to Yanan Wang who helped creating Fig. 1, and Anna Hennig who helped proofreading the paper.

References

- [1] Ejaz Ahmed, Michael Jones, and Tim K Marks. An improved deep learning architecture for person re-identification. In *Proceedings of the IEEE Conference on Computer Vision and Pattern Recognition*, pages 3908–3916, 2015. 1, 2
- [2] Yan Bai, Jile Jiao, Wang Ce, Jun Liu, Yihang Lou, Xuetao Feng, and Ling-Yu Duan. Person30k: A dual-meta generalization network for person re-identification. In *Proceedings of the IEEE/CVF Conference on Computer Vision and Pattern Recognition*, pages 2123–2132, 2021. 1, 3
- [3] Seokeon Choi, Taekyung Kim, Minki Jeong, Hyoungseob Park, and Changick Kim. Meta batch-instance normalization for generalizable person re-identification. In *Proceedings of the IEEE/CVF Conference on Computer Vision and Pattern Recognition*, pages 3425–3435, 2021. 3
- [4] Jiankang Deng, Jia Guo, Niannan Xue, and Stefanos Zafeiriou. Arcface: Additive angular margin loss for deep face recognition. In *Proceedings of the IEEE Conference on Computer Vision and Pattern Recognition*, pages 4690–4699, 2019. 2
- [5] Weijian Deng, Liang Zheng, Qixiang Ye, Guoliang Kang, Yi Yang, and Jianbin Jiao. Image-Image Domain Adaptation with Preserved Self-Similarity and Domain-Dissimilarity for Person Re-identification. In *Proceedings of the IEEE Computer Society Conference on Computer Vision and Pattern Recognition*, 2018. 1, 2
- [6] Yixiao Ge, Feng Zhu, Dapeng Chen, Rui Zhao, et al. Self-paced contrastive learning with hybrid memory for domain adaptive object re-id. *Advances in Neural Information Processing Systems*, 33:11309–11321, 2020. 7, 13
- [7] Ben Harwood, Vijay Kumar BG, Gustavo Carneiro, Ian Reid, and Tom Drummond. Smart mining for deep metric learning. In *Proceedings of the IEEE International Conference on Computer Vision*, pages 2821–2829, 2017. 3
- [8] K. He, X. zhang, S. Ren, and J. Sun. Deep residual learning for image recognition. In *Proceedings of IEEE Computer Society Conference on Computer Vision and Pattern Recognition*, pages 770–778, 2016. 5
- [9] Alexander Hermans, Lucas Beyrer, and Bastian Leibe. In defense of the triplet loss for person re-identification, 2017. 1, 2, 3, 4
- [10] Yang Hu, Dong Yi, Shengcai Liao, Zhen Lei, and Stan Z. Li. Cross dataset person Re-identification. In *ACCV Workshop on Human Identification for Surveillance (HIS)*, pages 650–664, 2014. 1, 3, 5
- [11] Qingqiu Huang, Yu Xiong, Anyi Rao, Jiase Wang, and Dahua Lin. Movienet: A holistic dataset for movie understanding. In *The European Conference on Computer Vision (ECCV)*, 2020. 14
- [12] Jieru Jia, Qiuqi Ruan, and Timothy M Hospedales. Frustratingly easy person re-identification: Generalizing person re-id in practice. In *British Machine Vision Conference*, 2019. 1, 3, 5
- [13] Xin Jin, Cuiling Lan, Wenjun Zeng, Zhibo Chen, and Li Zhang. Style Normalization and Restitution for Generalizable Person Re-identification. In *CVPR*, feb 2020. 1, 3, 5, 6
- [14] M Kostinger, Martin Hirzer, Paul Wohlhart, Peter M Roth, and Horst Bischof. Large scale metric learning from equivalence constraints. In *IEEE Conference on Computer Vision and Pattern Recognition*, 2012. 2
- [15] Wei Li, Rui Zhao, Tong Xiao, and Xiaogang Wang. Deep-ReID: Deep filter pairing neural network for person re-identification. In *IEEE Conference on Computer Vision and Pattern Recognition*, 2014. 1, 2, 5
- [16] Wei Li, Rui Zhao, Tong Xiao, and Xiaogang Wang. Deep-reid: Deep filter pairing neural network for person re-identification. In *Proceedings of IEEE Computer Society Conference on Computer Vision and Pattern Recognition*, 2014. 3, 11
- [17] Shengcai Liao, Yang Hu, Xiangyu Zhu, and Stan Z. Li. Person re-identification by local maximal occurrence representation and metric learning. In *IEEE Conference on Computer Vision and Pattern Recognition*, 2015. 2
- [18] Shengcai Liao and Ling Shao. Interpretable and Generalizable Person Re-Identification with Query-Adaptive Convolution and Temporal Lifting. In *European Conference on Computer Vision (ECCV)*, 2020. 1, 2, 3, 5, 6
- [19] Shengcai Liao and Ling Shao. TransMatcher: Deep Image Matching Through Transformers for Generalizable Person Re-identification. In *Advances in Neural Information Processing Systems*, 2021. 3, 7, 12, 14
- [20] W. Liu, Y. Wen, Z. Yu, M. Li, R. Bhiksha, and L. Song. Sphereface: Deep hypersphere embedding for face recognition. In *Proceedings of IEEE Computer Society Conference on Computer Vision and Pattern Recognition*, volume 1, page 1, 2017. 2
- [21] Xingang Pan, Ping Luo, Jianping Shi, and Xiaoou Tang. Two at once: Enhancing learning and generalization capacities via ibn-net. In *Proceedings of the European Conference on Computer Vision (ECCV)*, pages 464–479, 2018. 5
- [22] Xuelin Qian, Yanwei Fu, Tao Xiang, Yu-Gang Jiang, and Xiangyang Xue. Leader-based Multi-Scale Attention Deep Architecture for Person Re-identification. *TPAMI*, 2020. 1, 5, 6
- [23] Florian Schroff, Dmitry Kalenichenko, and James Philbin. Facenet: A unified embedding for face recognition and clustering. In *Proceedings of the IEEE conference on computer vision and pattern recognition*, pages 815–823, 2015. 2
- [24] Florian Schroff, Dmitry Kalenichenko, and James Philbin. FaceNet: A unified embedding for face recognition and clustering. In *Proceedings of the IEEE Computer Society Conference on Computer Vision and Pattern Recognition*, 2015. 3
- [25] Yantao Shen, Tong Xiao, Hongsheng Li, Shuai Yi, and Xiaogang Wang. End-to-end deep kronecker-product matching for person re-identification. In *Proceedings of the IEEE Conference on Computer Vision and Pattern Recognition*, pages 6886–6895, 2018. 1, 2
- [26] Evgeny Smirnov, Aleksandr Melnikov, Sergey Novoselov, Eugene Lukanets, and Galina Lavrentyeva. Doppelganger mining for face representation learning. In *Proceedings of the IEEE International Conference on Computer Vision Workshops*, pages 1916–1923, 2017. 3

- [27] Jifei Song, Yongxin Yang, Yi-Zhe Song, Tao Xiang, and Timothy M Hospedales. Generalizable person re-identification by domain-invariant mapping network. In *Proceedings of the IEEE Conference on Computer Vision and Pattern Recognition*, pages 719–728, 2019. [1](#), [3](#)
- [28] Yumin Suh, Bohyung Han, Wonsik Kim, and Kyoung Mu Lee. Stochastic class-based hard example mining for deep metric learning. In *Proceedings of the IEEE/CVF Conference on Computer Vision and Pattern Recognition*, pages 7251–7259, 2019. [3](#), [13](#)
- [29] Yumin Suh, Jingdong Wang, Siyu Tang, Tao Mei, and Kyoung Mu Lee. Part-aligned bilinear representations for person re-identification. *Proceedings of the European Conference on Computer Vision (ECCV)*, pages 402–419, 2018. [1](#), [2](#)
- [30] Yifan Sun, Liang Zheng, Yi Yang, Qi Tian, and Shengjin Wang. Beyond part models: Person retrieval with refined part pooling (and a strong convolutional baseline). In *Proceedings of the European Conference on Computer Vision (ECCV)*, 2018. [6](#)
- [31] Chong Wang, Xue Zhang, and Xipeng Lan. How to train triplet networks with 100k identities? In *Proceedings of the IEEE International Conference on Computer Vision Workshops*, pages 1907–1915, 2017. [3](#), [7](#), [13](#)
- [32] Guangrun Wang, Guangcong Wang, Xujie Zhang, Jianhuang Lai, Zhengtao Yu, and Liang Lin. Weakly supervised person re-id: Differentiable graphical learning and a new benchmark. *IEEE Transactions on Neural Networks and Learning Systems*, 32(5):2142–2156, 2020. [1](#)
- [33] Guanshuo Wang, Yufeng Yuan, Xiong Chen, Jiwei Li, and Xi Zhou. Learning discriminative features with multiple granularities for person re-identification. In *2018 ACM Multimedia Conference on Multimedia Conference*, pages 274–282. ACM, 2018. [6](#)
- [34] Yanan Wang, Shengcai Liao, and Ling Shao. Surpassing Real-World Source Training Data: Random 3D Characters for Generalizable Person Re-Identification. In *28th ACM International Conference on Multimedia (ACMMM)*, 2020. [1](#), [3](#), [5](#), [6](#), [14](#)
- [35] Longhui Wei, Shiliang Zhang, Wen Gao, and Qi Tian. Person transfer gan to bridge domain gap for person re-identification. In *Proceedings of the IEEE Conference on Computer Vision and Pattern Recognition*, pages 79–88, 2018. [5](#), [14](#)
- [36] Yandong Wen, Kaipeng Zhang, Zhifeng Li, and Yu Qiao. A discriminative feature learning approach for deep face recognition. In *European conference on computer vision*, pages 499–515. Springer, 2016. [2](#)
- [37] Chao-Yuan Wu, R Manmatha, Alexander J Smola, and Philipp Krahenbuhl. Sampling matters in deep embedding learning. In *Proceedings of the IEEE International Conference on Computer Vision*, pages 2840–2848, 2017. [3](#)
- [38] Mang Ye, Jianbing Shen, Gaojie Lin, Tao Xiang, Ling Shao, and Steven C. H. Hoi. Deep Learning for Person Re-identification: A Survey and Outlook. *arXiv preprint arXiv:2001.04193*, 2020. [2](#), [3](#)
- [39] Dong Yi, Zhen Lei, Shengcai Liao, and Stan Z. Li. Deep metric learning for person re-identification. In *International Conference on Pattern Recognition*, pages 34–39, Dec. 2014. [1](#), [2](#), [3](#), [5](#), [11](#)
- [40] Ye Yuan, Wuyang Chen, Tianlong Chen, Yang Yang, Zhou Ren, Zhangyang Wang, and Gang Hua. Calibrated Domain-Invariant Learning for Highly Generalizable Large Scale Re-Identification. *WACV*, pages 3578–3587, nov 2020. [3](#), [5](#), [6](#)
- [41] Tianyu Zhang, Lingxi Xie, Longhui Wei, Zijie Zhuang, Yongfei Zhang, Bo Li, and Qi Tian. Unrealperson: An adaptive pipeline towards costless person re-identification. In *Proceedings of the IEEE/CVF Conference on Computer Vision and Pattern Recognition*, pages 11506–11515, 2021. [6](#)
- [42] Yuyang Zhao, Zhun Zhong, Fengxiang Yang, Zhiming Luo, Yaojin Lin, Shaozi Li, and Nicu Sebe. Learning to generalize unseen domains via memory-based multi-source meta-learning for person re-identification. In *Proceedings of the IEEE/CVF Conference on Computer Vision and Pattern Recognition*, pages 6277–6286, 2021. [3](#), [5](#), [6](#)
- [43] L. Zheng, L. Shen, L. Tian, S. Wang, J. Wang, and Q. Tian. Scalable person re-identification: A benchmark. In *Proceedings of IEEE International Conference on Computer Vision*, 2015. [5](#)
- [44] Liang Zheng, Hengheng Zhang, Shaoyan Sun, Manmohan Chandraker, Yi Yang, and Qi Tian. Person re-identification in the Wild. In *Proceedings - 30th IEEE Conference on Computer Vision and Pattern Recognition, CVPR 2017*, 2017. [1](#), [2](#), [3](#)
- [45] Wei-Shi Zheng, Shaogang Gong, and Tao Xiang. Person re-identification by probabilistic relative distance comparison. In *Proceedings of IEEE Computer Society Conference on Computer Vision and Pattern Recognition*, pages 649–656, 2011. [2](#)
- [46] Zhun Zhong, Liang Zheng, Donglin Cao, and Shaozi Li. Re-ranking person re-identification with k-reciprocal encoding. In *Proceedings of the IEEE Conference on Computer Vision and Pattern Recognition*, pages 1318–1327, 2017. [5](#)
- [47] Kaiyang Zhou, Yongxin Yang, Andrea Cavallaro, and Tao Xiang. Omni-scale feature learning for person re-identification. In *Proceedings of the IEEE International Conference on Computer Vision*, 2019. [1](#), [3](#), [5](#), [6](#), [7](#), [12](#)
- [48] Kaiyang Zhou, Yongxin Yang, Andrea Cavallaro, and Tao Xiang. Learning generalisable omni-scale representations for person re-identification. *IEEE Transactions on Pattern Analysis and Machine Intelligence*, 2021. [5](#), [6](#)
- [49] Zijie Zhuang, Longhui Wei, Lingxi Xie, Tianyu Zhang, Hengheng Zhang, Haozhe Wu, Haizhou Ai, and Qi Tian. Rethinking the Distribution Gap of Person Re-identification with Camera-based Batch Normalization. In *ECCV*, pages 140–157, jan 2020. [1](#), [3](#), [5](#), [6](#)

Appendix

A. Pseudocode of the GS sampler

A pseudocode of the GS sampler is shown in Algorithm 1.

Algorithm 1: Graph Sampler

Input: Data source \mathbf{D} , feature extractor \mathbf{f} , pairwise distance function \mathbf{d} , batch size B , number of instances per class K .
Output: Sample iterator of the dataset \mathbf{D} .
Initialization: $pids$: list of all class IDs;
 $index_dict$: dictionary of list containing all sample indices of each class.
Procedure:
index = []
for p in $pids$:
 index.append(random.choice($index_dict[p]$, size=1)) # randomly select one sample per class
dataset = $\mathbf{D}(index)$ # construct a small sub-dataset
 $X = \mathbf{f}(\text{dataset})$ # extract features
dist = $\mathbf{d}(X, X)$ # calculate pairwise distance
dist[i,i] = Inf # ignore the diagonal elements
 $P = B / K$ # number of classes in a mini batch
topk_index = topk(-dist, size= $P-1$) # find nearest neighboring classes
index = []
for p in shuffle($pids$):
 index.extend(random.choice($index_dict[p]$, size= K)) # randomly select K samples per class
 for k in topk_index[p]:
 index.extend(random.choice($index_dict[k]$, size= K)) # randomly select K samples per class
Return: iter(index)

B. Alternative Loss Function and Analysis

B.1. Binary Cross Entropy Loss

Note that the batch hard triplet loss (Eq. (1) in the main paper) is usually used as an auxiliary to the classification loss, but not alone, in person re-identification. This is probably because random samplers including PK cannot provide informative mini batches for OHEM to mine, which makes Eq. (1) very small or even zero, and so the learning is not efficient. In contrast, with the proposed GS sampler, we prove that the OHEM triplet loss works well by itself with $K = 2$. We use this loss function alone because, as motivated in the main paper, we aim at removing classification layers for large-scale metric learning.

However, note that the GS sampler already provides almost the hardest mini batches, and the batch hard triplet loss further finds the hardest triplets within a mini batch for training. As a result, the model may suffer optimization difficulty, which in turn may impact convergence during training. In practice, we find that limiting $K = 2$ alleviates this problem significantly, while $K > 2$ usually makes the learning not able to converge.

Alternatively, pairwise verification or binary classification is another solution [3,9] for pairwise matching or metric learning within mini batches. Specifically, we apply QAConv to compute similarity values between a pair of images, and formulate a pairwise verification or binary classification problem in mini-batch based learning. Accordingly, we compute the binary cross entropy loss as follows.

$$\ell(\theta) = -\frac{1}{B} \sum_{i=1}^B \sum_{j \neq i} y_{ij} \log(p_{ij}(\theta)) + (1-y_{ij}) \log(1-p_{ij}(\theta)), \quad (\text{B})$$

where B is the mini-batch size, θ is the network parameter, $p_{ij} \in [0, 1]$ is the QAConv similarity indicating binary classification probability, and $y_{ij} = 1$ indicates a positive pair, while a negative pair otherwise. By default, we choose $B = 64$ and $K = 4$ for this loss.

B.2. Experimental Comparison

Table D shows a comparison between the hard triplet loss and the binary cross entropy loss for QAConv-GS. Results shown in the table indicate that, the hard triplet loss performs better than the binary cross entropy loss for all datasets, thanks to OHEM which further mines hard examples within mini batches provided by GS. However, the hard triplet loss used alone in the proposed pipeline is sensitive to K values as discussed. In contrast, the binary cross entropy loss is a more stable alternative, working well with different B and K values. This will be analyzed in the following subsection.

B.3. Parameter analysis

When the binary cross entropy loss is applied, in Fig. E, we show the performance with different parameter configurations of the GS sampler, trained on Market-1501. We observe that for the batch size (Fig. E (a)), generally the accuracy increases with the increasing batch size (thus increasing P), but saturates at about 64. It is understood that mini batches with larger batch size provides more comprehensive data for learning, however, at the cost of enlarged computation time, recalling that the number of iterations per epoch is fixed as C for the GS sampler. For example,

Train	Method	CUHK03		Market		MSMT17	
		R1	mAP	R1	mAP	R1	mAP
Market	Binary	16.4	15.7	-	-	41.2	15.0
	Triplet	19.1	18.1	-	-	45.9	17.2
MSMT	Binary	20.0	19.2	75.1	46.7	-	-
	Triplet	20.9	20.6	79.1	49.5	-	-
MS-all	Binary	27.2	27.1	80.6	55.6	-	-
	Triplet	27.6	28.0	82.4	56.9	-	-
RP	Binary	14.8	13.4	74.0	43.8	42.4	14.4
	Triplet	18.4	16.1	76.7	46.7	45.1	15.5

Table D. Comparison of loss functions. Binary: binary cross entropy loss. Triplet: hard triplet loss. Market: Market-1501 dataset. MSMT: MSMT17 dataset. MS-all: MSMT17 (all). RP: RandPerson dataset.

with $B = 64$, the training of QAConv-GS on Market-1501 is about 0.68 hours on a single V100 GPU. However, this is about 1.32 hours with $B = 128$ for training the same epochs.

Next, we evaluate the influence of K under fixed $B = 64$, as shown in Fig. E (b). Interestingly, larger K leads to gradually better performance on the CUHK03-NP, however, it degrades the performance significantly on MSMT17. It appears that $K = 4$ is a reasonable trade-off.

Since the hard triplet loss performs better, in the following, by default we still use this loss.

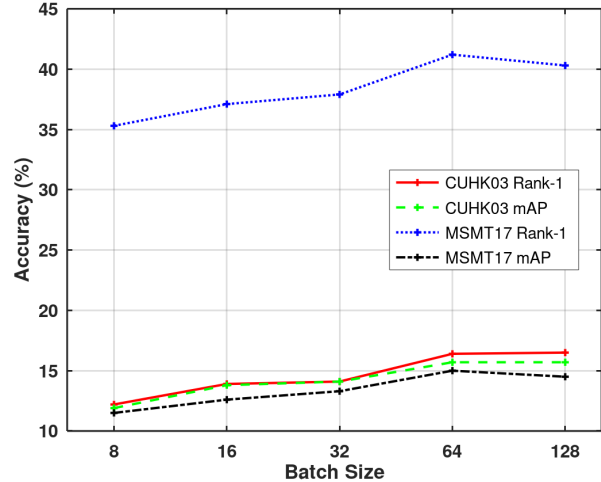
C. Application to Other Baselines

Furthermore, to show the generality of the proposed graph sampling method, we apply it to two other algorithms, namely OSNet [10] and TransMatcher [4].

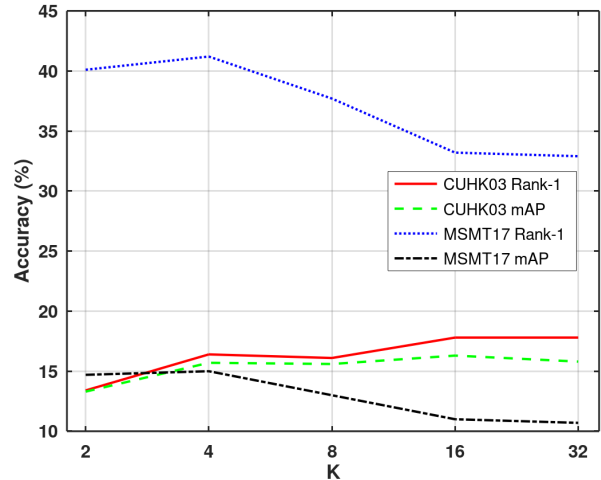
The official code of OSNet² (MIT License) is used. We used its osnet_ibn_x1_0 config, with softmax+triplet loss and the PK sampler (RandomIdentitySampler) for the best performance, denoted by OSNet-IBN + PK. This combination of softmax+triplet loss and the PK sampler is also the most popular setting in person re-identification for strong baselines. Then, upon this baseline, we apply the proposed graph sampling to replace the PK sampler, denoted by OSNet-IBN + GS. The training is performed on the MSMT17 (all), as in [10], and the learned models are evaluated on the CUHK03-NP and Market-1501 datasets. The results are shown in Table E. From the comparison it can be seen that the proposed GS sampler can also improve other strong baselines in replacing the popular PK sampler. Therefore, it is proved to be general and may also be applied to other methods.

Furthermore, with a very recent method TransMatcher

²<https://github.com/KaiyangZhou/deep-person-reid>



(a) Effect of batch size



(b) Effect of K

Figure E. Performance with different parameter configurations of the GS sampler when the binary cross entropy loss is applied, trained on Market-1501. (a) with varying batch size under fixed $K = 4$; and (b) with varying K under fixed $B = 64$.

Table E. Direct cross-dataset evaluation results (%) with different baselines trained on MSMT17 (all).

Method	CUHK03		Market	
	R1	mAP	R1	mAP
OSNet-IBN [10]	-	-	66.5	37.2
OSNet-IBN + PK	23.4	23.6	67.9	39.6
OSNet-IBN + GS	24.5	24.9	71.3	42.6

[4], we also compare the PK and GS samplers. The official code of TransMatcher³ (MIT License) is used, with its de-

³<https://github.com/ShengcaiLiao/QAConv/tree/master/projects/transmatcher>

fault settings. The results are shown in Table F. It can also be observed that on average the proposed GS sampler performs much better than the PK sampler, verifying again the generality of GS.

D. Application to Unsupervised Domain Adaptation

As a new scenario, we tried unsupervised domain adaptation (UDA) by replacing PK with GS in the source domain of SpCL [1]. The Rank1/mAP results for PK and GS are 86.1/70.9 and 87.3/71.5, respectively, for CUHK03-NP→Market-1501. Slight improvements can be observed. However, for the time being, it is still not yet straightforward to apply GS for pseudo labeled samples by clustering on the target domain. This may be because pseudo labels could be noisy, and GS may be aggressive in finding hard negative samples that could possibly be positive. To address this, further developments may be required in considering how to handle noisy samples, which is quite interesting.

E. Further Ablation Studies

In this paper, all experiments are with images of 384×128 as inputs. To understand the influence of image size, we also conduct experiments with images of 256×128 as inputs. The results are shown in Table G. It can be seen that the results are quite close to each other on Market-1501 and MSMT17, though results with 384×128 are clearly better than that of 256×128 on CUHK03. Note that our results with 256×128 still achieve the state of the art compared to existing methods in Table 1 of the main paper.

In the proposed GS, one example per class is sampled for the graph construction, which is efficient. Alternatively, class centers can also be considered for graph construction. In fact, class centers are used in [6] for clustering based batch sampling, and we show better performance of GS in Table 3 of the main paper. To further understand this, we use class centers to construct graphs for GS. This is denoted by QAConv-GS-Center. The comparison results are shown in Table G. It is clear that GS performs better.

There might be two problems with class centers. First, it lacks flexibility of sample relationships, since many classes may have large distribution variances. This is also discussed in [5]. Second, computing class centers requires feature extraction of all training samples, which hinders large-scale learning. The average training time increases from 1.68 hours of QAConv-GS to 2.27 hours of QAConv-GS-Center. Especially, QAConv-GS costed 3.4 hours to train MSMT17 (all), but QAConv-GS-Center costed 5.4 hours.

F. Visualization of GS

Finally, we show some examples for the nearest neighboring classes generated by the GS sampler in Fig. F. It

can be observed that, the GS sampler is indeed able to find similar classes as hard examples to challenge the learning. For example, similar kind of clothes, similar colors, patterns, and accessories. These confusing examples helps a lot in learning discriminative models. Besides, it seems that in early epochs, the model tends to evaluate similarity with visual appearance, regardless of the influence of foreground and background. However, in late epochs, the model learns to remove the influence of background, and learns higher level of abstraction. For example, in the upper right group, the similarity is less affected by bicycles in background with epoch 15. In the first group of MSMT17, the similarity is less affected by trees in background with later epochs. With epoch 15 of the first group, the model learns the concept of security guards. In the upper right group, with epoch 15 the model learns the concept of girls with short skirts. In the last group of Market-1501, with epoch 15 the clothes are more consistent in style and color. In the upper right group of MSMT17, with epoch 15 in GS the model correctly retrieves red coats. In the last group of MSMT17, with epoch 15 in GS the model correctly retrieves pink coats as well.

G. Limitations

The proposed method, despite achieving very good results, may have two limitations. First, GS requires additional computation for mini batch sampling. We design two ways to reduce the computation, that is, employing GS only at the beginning of each epoch, and randomly sampling only one sample per class for the distance computation and graph construction. As a result, the additional running time introduced by GS is still acceptable, as reported in Section 5.4.1 of the main paper. Besides, note that with GS the number of training epochs is generally reduced. For example, with GS the proposed method usually requires less than 20 epochs for training, while existing methods typically require 60 epochs or more to train. Therefore, GS deserves the additional computational costs. However, in our experiments, the maximal number of classes is only 8,000. GS may still have a big limitation with millions of identities, which need further investigation.

Second, as discussed, GS provides challenging examples for training, and so the default hard triplet loss only works well with $K = 2$. Otherwise, the training is too difficult to converge. Nevertheless, as discussed in Section B, this limitation can be solved by employing the binary cross entropy loss as an alternative, though with inferior performance.

H. Social Impacts

Person re-identification is a technique to automatically search persons from a large amount of videos. It has potential social values in some practical applications, such as person image retrieval of suspects, character recognition in

Method	Training	CUHK03-NP		Market-1501		MSMT17	
		Rank-1	mAP	Rank-1	mAP	Rank-1	mAP
TransMatcher-PK	Market-1501	22.9	21.5	-	-	45.6	17.8
TransMatcher-GS	Market-1501	22.2	21.4	-	-	47.3	18.4
TransMatcher-PK	MSMT17	23.6	22.9	78.3	51.7	-	-
TransMatcher-GS	MSMT17	23.7	22.5	80.1	52.0	-	-
TransMatcher-PK	MSMT17 (all)	30.7	29.5	79.9	55.7	-	-
TransMatcher-GS	MSMT17 (all)	31.9	30.7	82.6	58.4	-	-
TransMatcher-PK	RandPerson	18.0	16.5	73.3	45.3	40.6	14.1
TransMatcher-GS	RandPerson	17.1	16.0	77.3	49.1	48.3	17.7

Table F. Comparison of direct cross-dataset evaluation results (%) using TransMatcher [4] with PK and GS. MSMT17 (all) means all images are used for training, regardless of subset splits.

Method	Training	CUHK03-NP		Market-1501		MSMT17	
		Rank-1	mAP	Rank-1	mAP	Rank-1	mAP
QAConv-GS	Market-1501	19.1	18.1	-	-	45.9	17.2
QAConv-GS (256 × 128)	Market-1501	16.9	17.2	-	-	45.4	17.1
QAConv-GS-Center	Market-1501	15.4	14.7	-	-	45.0	15.7
QAConv-GS	MSMT17	20.9	20.6	79.1	49.5	-	-
QAConv-GS (256 × 128)	MSMT17	18.6	19.8	77.9	49.6	-	-
QAConv-GS-Center	MSMT17	15.3	16.1	73.9	41.5	-	-
QAConv-GS	MSMT17 (all)	27.6	28.0	82.4	56.9	-	-
QAConv-GS (256 × 128)	MSMT17 (all)	24.3	25.6	81.5	55.3	-	-
QAConv-GS-Center	MSMT17 (all)	25.2	24.6	78.6	51.2	-	-
QAConv-GS	RandPerson	18.4	16.1	76.7	46.7	45.1	15.5
QAConv-GS (256 × 128)	RandPerson	16.2	14.4	74.7	45.5	45.0	15.8
QAConv-GS-Center	RandPerson	17.4	15.4	76.8	47.0	44.3	15.2

Table G. Comparison of the direct cross-dataset evaluation results (%) for different variants of QAConv-GS. QAConv-GS-Center is based on selecting class centers for graph construction for GS. MSMT17 (all) means all images are used for training, regardless of subset splits.

movies [2], and so on. For example, it is very useful to reduce large amount of human labors and greatly advance the effort in criminal investigation. Accordingly, person re-identification methods are actively studied. The person re-identification technique, however, may also be used by company for a surveillance of employees, or by malls for tracking of daily visitors. Therefore, it requires effective legislation to avoid abuse of this technique. This paper focuses on foundational research; it is not tied to particular applications, let alone deployments.

Besides, the research and developments of such technique are often with datasets collected from surveillance videos that may contain personally identifiable information. To address this, a positive action is to remove such information, as done in MSMT17v2 [8] with facial areas masked. More promisingly, a better way recently demonstrated is to use synthesized data, as done in RandPerson [7].

References

- [1] Yixiao Ge, Feng Zhu, Dapeng Chen, Rui Zhao, et al. Self-paced contrastive learning with hybrid memory for domain adaptive object re-id. *Advances in Neural Information Processing Systems*, 33:11309–11321, 2020. **7, 13**
- [2] Qingqiu Huang, Yu Xiong, Anyi Rao, Jiase Wang, and Dahua Lin. Movienet: A holistic dataset for movie understanding. In *The European Conference on Computer Vision (ECCV)*, 2020. **14**
- [3] Wei Li, Rui Zhao, Tong Xiao, and Xiaogang Wang. Deep-reid: Deep filter pairing neural network for person re-identification. In *Proceedings of IEEE Computer Society Conference on Computer Vision and Pattern Recognition*, 2014. **3, 11**
- [4] Shengcai Liao and Ling Shao. TransMatcher: Deep Image Matching Through Transformers for Generalizable Person Re-identification. In *Advances in Neural Information Processing Systems*, 2021. **3, 7, 12, 14**
- [5] Yumin Suh, Bohyung Han, Wonsik Kim, and Kyoung Mu Lee. Stochastic class-based hard example mining for deep



Figure F. Eight groups of examples for the nearest neighboring classes generated by the GS sampler. The first two rows are from the training on Market-1501, while the last two rows are from that of MSMT17. In each group, three sets of images are shown, corresponding to epoch 2, 8, and 15. In each set, the upper left image is the center class, and other images are the top-7 nearest neighboring classes to the center class.

- metric learning. In *Proceedings of the IEEE/CVF Conference on Computer Vision and Pattern Recognition*, pages 7251–7259, 2019. [3](#), [13](#)
- [6] Chong Wang, Xue Zhang, and Xipeng Lan. How to train triplet networks with 100k identities? In *Proceedings of the IEEE International Conference on Computer Vision Workshops*, pages 1907–1915, 2017. [3](#), [7](#), [13](#)
- [7] Yanan Wang, Shengcai Liao, and Ling Shao. Surpassing Real-World Source Training Data: Random 3D Characters for Generalizable Person Re-Identification. In *28th ACM International Conference on Multimedia (ACMMM)*, 2020. [1](#), [3](#), [5](#), [6](#), [14](#)
- [8] Longhui Wei, Shiliang Zhang, Wen Gao, and Qi Tian. Person transfer gan to bridge domain gap for person re-identification. In *Proceedings of the IEEE Conference on Computer Vision and Pattern Recognition*, pages 79–88, 2018. [5](#), [14](#)
- [9] Dong Yi, Zhen Lei, Shengcai Liao, and Stan Z. Li. Deep metric learning for person re-identification. In *International Conference on Pattern Recognition*, pages 34–39, Dec. 2014. [1](#), [2](#), [3](#), [5](#), [11](#)
- [10] Kaiyang Zhou, Yongxin Yang, Andrea Cavallaro, and Tao Xiang. Omni-scale feature learning for person re-identification. In *Proceedings of the IEEE International Conference on Computer Vision*, 2019. [1](#), [3](#), [5](#), [6](#), [7](#), [12](#)

Biography

Shengcai Liao is the Director of Research and Developments (Acting) in the Inception Institute of Artificial Intelligence (IIAI), Abu Dhabi, UAE. He is a Senior Member of IEEE. Previously, he was an Associate Professor in the Institute of Automation, Chinese Academy of Sciences (CASIA). He received the B.S. degree in mathematics from the

Sun Yat-sen University in 2005 and the Ph.D. degree from CASIA in 2010. He was a Postdoc in the Michigan State University during 2010-2012. His research interests include object detection, recognition, and tracking, especially face and person related tasks. He has published over 100 papers, with **15,800+ citations and h-index 44** according to Google Scholar. He **ranks 905 among 215,114 scientists (Top 0.42%)** in 2019 single year in the field of AI, according to a study by Stanford University of Top 2% worldwide scientists. His representative work LOMO+XQDA, known for effective feature design and metric learning for person re-identification, has been **cited 2,000+ times and ranks top 10 among 602 papers in CVPR 2015**. He was awarded/co-awarded the Best Student Paper in ICB 2006, ICB 2015, and CCBR 2016, and the Best Paper in ICB 2007. He was also awarded the IJCB 2014 Best Reviewer and CVPR 2019/2021 Outstanding Reviewer. He was an Assistant Editor for the book “Encyclopedia of Biometrics (2nd Ed.)”. He serves as Program Chair for IJCB 2022. He served as Area Chairs for ICPR 2016, ICB 2016 and 2018, and CVPR 2022, SPC for IJCAI 2021, and reviewers for ICCV, CVPR, ECCV, NeurIPS, ICLR, AAAI, TPAMI, IJCV, TIP, etc. His team was the Winner of the CVPR 2017 Detection in Crowded Scenes Challenge and ICCV 2019 NightOwls Pedestrian Detection Challenge. Home-page: <https://liaosc.wordpress.com/>